Direct Calculation of High-Speed Cavity Flows in a Scramjet Engine by the CESE Method

Chang-Kee Kim[1], Kyoung-Su Im[2], S.- T. John Yu[3]
Mechanical Engineering Department
Wayne State University, Detroit, MI 48202

Abstract

In this paper we apply the Space-Time CESE method to simulate supersonic flows over open cavities, in the setting of a dual-mode scramjet engine to enhance fuel/air mixing and flame holding. Detailed flow features of cavity flows with and without an upstream injection are successfully captured. The present numerical results compared favorably with the experimental data for dominant frequencies and time-averaged pressure coefficients inside the cavities. With an upstream injection, the flow oscillations are drastically suppressed. The present results show that the CESE method is a viable CFD approach for high fidelity simulations of unsteady flows relevant to advanced scramjet engine concepts.

1. Introduction

Fuel injection, ignition, and flame holding are challenging issues in designing a scramjet engine. A successful fuel injection method must provide rapid fuel/air mixing with minimum total-pressure loss in the air stream. A stable flame-holding system for a wide range of operating conditions is critical to the engine performance.

The AF supersonic combustion testing facilities in WPAFB [1, 2] provide a prototype of a next-generation, dual-mode, hydrocarbon fueled scramjet engine. Inside the combustor, various cavity flame holders have been tested in conjunction with flush-wall and parallel fuel injection schemes.

Cavity flows is composed of complex flow features of boundary layer separation, shear layer instability, vortices shedding, and acoustic waves. Unsteady oscillations occur under a wide range of flow conditions and cavity geometries. Recent studies showed that the oscillations are useful to enhance fuel/air mixing and to stabilize the flame with acceptable pressure loss [3, 4, 5]. Behaviors of cavity flows and the associated acoustic waves, however, can be drastically changed by the fuel injection mechanism employed. Many times, the inherent oscillations of cavity flows may disappear [3, 9, 10, 11].

In the past, extensive experimental and theoretical studies on flows over cavities have been conducted. Fundamental characteristics such as the oscillation frequency have been reported, e.g., [6-8]. However, it is difficult to directly apply this knowledge to scramjet engine design due to the additional complexity of fuel injection and different flow regimes of interest. In particular, a viable modeling tool is needed to assess the amplitude of pressure oscillations and dominant frequency modes in the scramjet engine.

The objective of the present paper is to demonstrate the capabilities of the Space-Time Conservation Element and Solution Element (CESE) Method in calculating the highly unsteady cavity flows with and without the fuel injection mechanism, in a setting of a typical scramjet engine, e.g., the AF testing facilities [1, 2]. The experience and knowledge so gained could be a steppingstone to further explore the use of the novel CESE method for simulations of more

[1] Research associate, AIAA member, Email: ckkim@fluid.eng.wayne.edu
[2] Research Assistant Professor, AIAA Member, Email: ksim@fluid.eng.wayne.edu
[3] Associate Professor, AIAA Member, Email: styu@eng.wayne.edu

complex flows relevant to advanced concepts in the further development of scramjet engines.

The rest of the paper is organized in the following. In Section 2, we briefly review the model equations to be solved by the CESE method. Section 3 provides background information of the CESE method. Section 4 shows numerical solutions by the CESE method, including detailed comparison between the present numerical results and the experimental data for oscillating frequencies and time averaged pressure coefficient on the cavity floor. We then show results of interactions between an upstream injection and a cavity flow. Finally, we offer concluding remarks and provide cited references.

2. Governing Equations

The two-dimensional Navier-Stokes equations for compressible flows in Cartesian coordinates are presented in a vector form:

$$\frac{\partial \mathbf{U}}{\partial t}+\frac{\partial \mathbf{F}}{\partial x}+\frac{\partial \mathbf{G}}{\partial y}-\frac{\partial \mathbf{F}_v}{\partial x}-\frac{\partial \mathbf{G}_v}{\partial y}=0 \qquad (1)$$

where **U** is the flow variable vector, **F** and **G** are the inviscid flux vectors, and $\mathbf{F}_v$, and $\mathbf{G}_v$ are the viscous flux vectors:

$$\mathbf{U}=\begin{pmatrix}\rho\\ \rho u\\ \rho v\\ \rho e\end{pmatrix},\ \mathbf{F}=\begin{pmatrix}\rho u\\ \rho u^2+p\\ \rho uv\\ u(\rho e+p)\end{pmatrix},\ \mathbf{G}=\begin{pmatrix}\rho v\\ \rho uv\\ \rho v^2+p\\ v(\rho e+p)\end{pmatrix}$$

$$\mathbf{F}_v=\begin{pmatrix}0\\ \tau_{xx}\\ \tau_{xy}\\ u\tau_{xx}+v\tau_{xy}-q_x\end{pmatrix},$$

$$\mathbf{G}_v=\begin{pmatrix}0\\ \tau_{xy}\\ \tau_{yy}\\ u\tau_{xy}+v\tau_{yy}-q_y\end{pmatrix}$$

where ρ is density; u and v are velocity components in the x and the y directions, respectively; p is pressure; $e = \varepsilon + 1/2(u^2 + v^2)$ is the specific total energy with ε as the internal energy. Note that due to the ideal gas equation, $p=(\gamma - 1)\rho\ \varepsilon$, and $\gamma = Cp/Cv$ is the specific hear ratio. In the viscous vectors, τ_{xx}, τ_{xy}, τ_{yx}, and τ_{yy} are shear stresses, and q_x and q_y are the x and the y components of the heat conduction flux, respectively.

The above governing equations are non-dimensionalized by the free stream conditions, i.e., velocity components u and v by u_∞; density by ρ_∞; pressure by $\rho_\infty u_\infty^2$; and the total energy e by $\rho_\infty u_\infty^2$. The cavity depth D is used as the length scale for nondimensionalization, and the time scale is D/u_∞.

3. The CESE Method

The Space-Time Conservation Element Solution Element (CESE) Method, originally proposed by Chang [12, 13, 14, 15], is distinguished by the simplicity of its conceptual basis, i.e., flux conservation in space and time and a unified treatment of space and time in enforcing flux conservation. As a contrast to modern upwind schemes, no Riemann solver or reconstruction procedure is used, and the logic and rational of the present method is extremely simple. No directional splitting or fractional step method is used in the CESE method, and numerical accuracy does not deteriorate as we change from one-dimensional calculations to multi-dimensional ones.

In the CESE method, we reformulate Eqn. (1) by letting $x_1 = x$, $x_2 = y$, and $x_3 = t$. The space-time domain of interest in the present calculation becomes a three-dimensional Euclidean space E_3. As a result, Eqn. (2) could be represented as

$$\nabla \cdot \mathbf{h}_i = 0\,, \qquad (2)$$

for $i = 1, 2, 3,$ and 4 for the four equations. The space-time flux vector $\mathbf{h}_i = [(f - f_v)_i,\ (g - g_v)_i,\ u_i]^T$. Note that $(f - f_v)_i$ and $(g - g_v)_i$ are ith component of $\mathbf{F}$-$\mathbf{F}_v$ and $\mathbf{G}$-$\mathbf{G}_v$, respectively. By Gauss' divergence theorem,

$$\oint_{S(V)} \mathbf{h}_i \cdot d\vec{\mathbf{s}} = 0 \qquad (3)$$

where V is a space-time volume, $S(V)$ is the surface of V, and $d\vec{\mathbf{s}}$ is a surface element vector pointing outward. Figure 1 shows an arbitrary space-time volume in one spatial dimension. By introducing separated definition for conservation element and

solution element, the CESE method integrates Eqn. (3) and march the solution forward in time. Computer programs solving one-, two- and three-dimensional flow equations have developed. The CESE computer programs can solve structured and unstructured meshes, composed of triangles and quads for two-dimensional problems and tetrahedrons, prisms, pyramids, and hexes for three-dimensional problems.

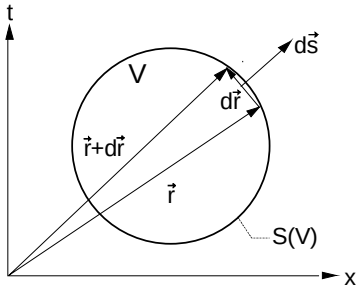

Fig. 1: A schematic of space-time integral of the CESE method.

Previously, by using the CESE method, we have reported numerical results of detonation waves, cavitations, low-Mach-number viscous flows, various acoustic problems, and plume dynamics of a pulse detonation engine (PDE). We also found that the CESE solver is capable of calculating high-speed compressible flow as well as flows at very low Mach numbers without applying preconditioning to the flow equations. The CESE method is indeed a promising new numerical framework for unsteady fluid mechanics at all speeds.

The boundary condition treatments in the CESE method is constructed based on space-time flux conservation in the vicinity of the computational boundary, including the reflective, non-reflective, and solid-wall boundary conditions. In particular, in the setting of the space-time flux conservation, i.e., Eqn. (3), the implementation of a non-reflective boundary condition is extremely simple due to the fact that all fluid information must propagate into the future. Along a wall boundary, Chang and co-works developed a unified boundary condition for both inviscid and viscous flows. A non-slip condition will be automatically enforced when the viscosity is not null.

4. Results and Discussion

Three numerical examples are presented here (1) an AF testing condition for evaluating the accuracy of the calculated frequency, (2) a NASA testing condition for evaluation of the accuracy of time-averaged amplitudes of pressure fluctuations along the cavity walls, and (3) preliminary results of a cavity flow with an upstream transverse injection.

4.1 AF Testing Case

Our first numerical example follows the testing condition in the AF facility reported in [4]. A supersonic flow at Mach 2 and Reynolds number of 4.5×10^7 (per meter) passes a swallow cavity, in which L/D = 7.76. L and D are the length and depth of the cavity, respectively. The computational domain after non-dimensionalization is $0 \le x \le 11.52$, and $0 \le y \le 3.82$. Mesh points were clustered at the forward and aft bulkheads, at the plane of the mouth, and along the lateral sidewalls. 143,000 triangular elements are used in the domain. The inlet boundary condition was assumed uniform. The unified boundary condition is applied to the solid wall. The non-reflective boundary condition is applied to the free stream surface and outlet. Initially, velocities inside the cavity are set to zero, and the density and pressure of the whole domain are set to the free stream values. The time step was chosen such that CFL ≈ 0.8.

Figure 2 shows a series of snapshots of pressure contours, vorticity contours, and numerical Schlieren images. The numerical Schlieren image is the contour plots of

$$|\nabla\rho| = \sqrt{\left(\frac{\partial\rho}{\partial x}\right)^2 + \left(\frac{\partial\rho}{\partial y}\right)^2} \qquad (4)$$

These figures demonstrate very complex flow features, including traveling acoustic waves, vortex generation at the leading edge, shedding vortices in the shear layer, and pressure waves impinging on and rebounding from the aft wall. These mechanisms form self-sustained oscillations, which are consistent with the feed back loop suggested by Rossiter [7].

From Fig. 2(b), the shear layer fluctuations could be clearly discerned. Inward deflection of the

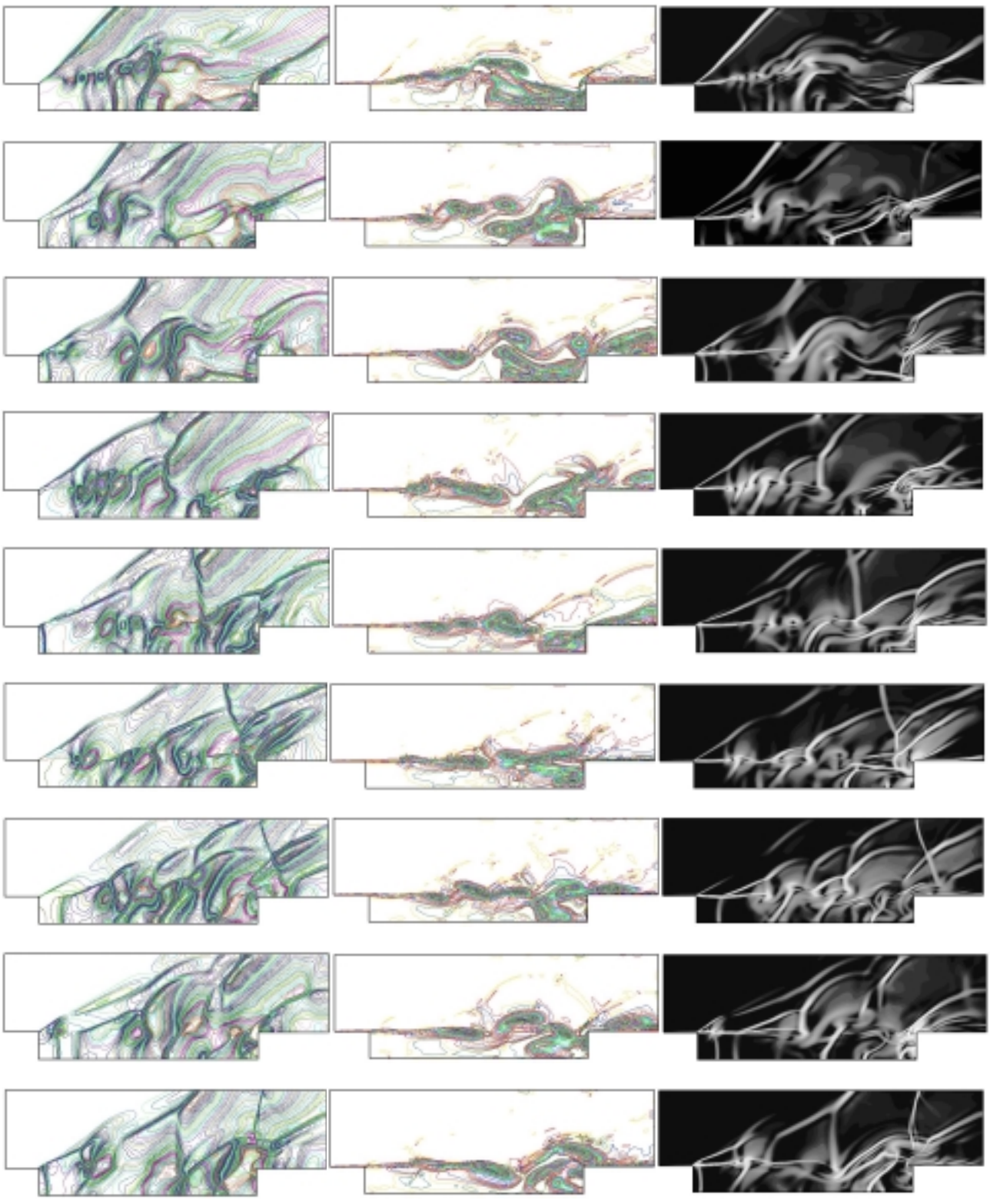

(a) (b) (c)

Fig. 2: Snapshots of flow fields of a cavity flow with M=2.0, L/D=7.76,
(a) pressure contours, (b) vorticity contours, and (c) numerical Schlieren images

shear layer results in mass addition into the cavity. On the other hand, outward deflection of the shear layer allows mass expulsion from the cavity. This periodic mass addition/expulsion could be critical to the fuel/air mixing and flame-holding in scramjet engine applications. Moreover, a resonating shock wave above the cavity, shown in Fig. 2 (c), can also enhance fuel/air mixing.

Figure 3 shows the pressure history at locations on the aft wall and on the floor. The flow has reached a semi self-sustained oscillatory state after about 15 t_c. Note $t_c = D/ U_\infty$. However, the oscillation pattern changes from cycle to cycle, and one cannot clearly identify the period of the oscillation cycles. This is consistent with experimental observation reported in [8]. The amplitude of the pressure oscillations at the aft wall is much higher than that at the cavity floor due to the mass addition and expulsion mechanism along the aft wall.

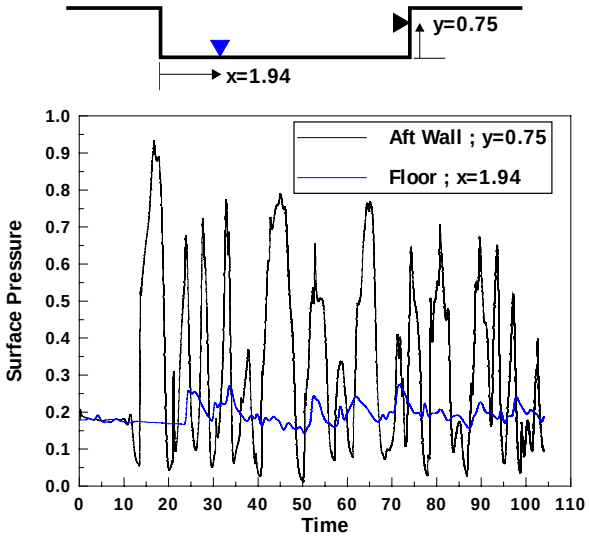

Fig. 3: Monitored pressure history on the wall inside the cavity for Mach 2.0 and L/D=7.76

Figure 4 shows its frequency spectra of the pressure oscillations shown in Fig. 3. The predicted values of the dominant frequencies compare well with the Rossiter relation, and the numerical results by Baurle et al. [4]. The Rossiter formula is

$$f_m = \left(\frac{U}{L}\right)\frac{m-\alpha}{(K)^{-1}+M_\infty\left(T/T_o\right)^{\frac{1}{2}}} \qquad (5)$$

where f_m is the resonant frequency corresponding to the m^{th} mode, U is the main stream velocity, L is the cavity length, α= 0.513, and K= 0.57. The calculated dominant frequencies are 574, 2294, 3441, and 5735Hz, which compare well with the 1st, 3rd, 4th, and 6th mode by the Rossiter relation.

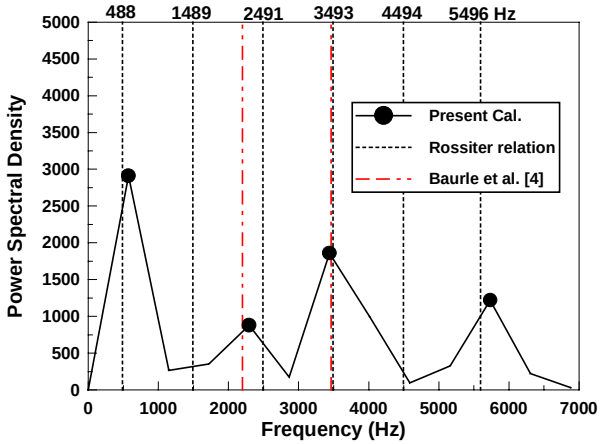

Fig. 4: The predicted frequencies for the cavity flow with in the AF testing case.

4.2 NASA Testing Case

The validation of the numerical calculations for the amplitudes of pressure oscillations is performed by using the experimental data reported in [16]. In this testing case, a free stream at Mach 1.5 flows over an open cavity with L/D = 6.0.

Figure 5 shows the comparison between the present numerical solutions and the experimental data for the time-averaged pressure coefficient, which is defined as

$$c_p = 2\left(\bar{p} - \frac{1}{\gamma M_\infty^2}\right) \qquad (6)$$

where $\bar{p}$ is the time-averaged surface pressure.

The calculated results for both inviscid and viscous flows are in good agreement with the experimental data. The discrepancy near the fore wall is probably due to uncertainties of the incoming boundary layer in the experiments.

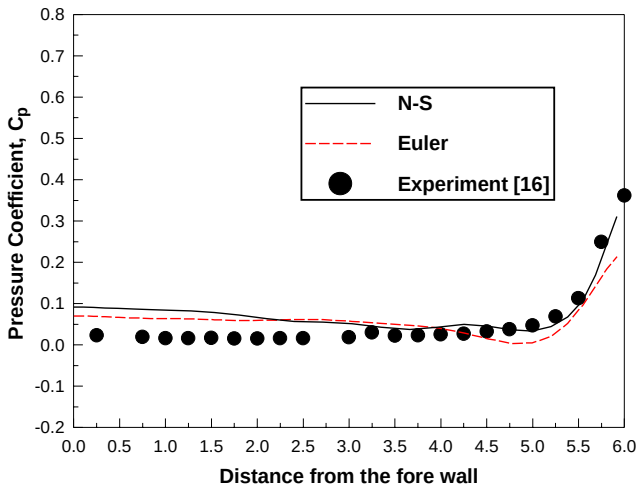

Fig. 5: Time-averaged pressure coefficients along the cavity floor in the NASA testing case.

4.3 Cavity with Upstream Injection

As the last numerical example, we consider a cavity flow with an upstream injection in the transverse direction. The calculation domain is $0 \le x \le 13.80$, $0 \le y \le 4.0$, which is decomposed into 45,200 triangular elements. The free stream flow condition and the cavity geometry are identical to that of the Case 1. The injection jet opening is 0.2 D, and its center is located 1.0 D upstream from the leading edge at forward bulkhead. A choked jet with a uniform condition at the opening imposed with $J = 1.0$, $p_j / p_\infty = 4.34$, $\rho_j / \rho_\infty = 6.593$, where

$$J = (\rho u^2)_{jet} / (\rho u^2)_{freestream} \qquad (7)$$

is the ratio of stream momentum fluxes of jet and the free stream.

Figure 6 shows the time histories of pressure oscillations with and without upstream injection at the fore wall and aft wall locations. When the injection is turned on, flow oscillations inside the cavity are suppressed, and the oscillation pattern is changed. This result is qualitatively consistent with that reported by Vakili et al. [9].

Figure 7 shows the frequency spectrum of pressure oscillations on the aft wall location. The calculated dominant frequencies are 315, 1893, 2523, 3470 and 5735Hz. Comparing with the frequencies shown in Fig. 4, we conclude that upstream injection causes the dominant frequencies shift to lower values.

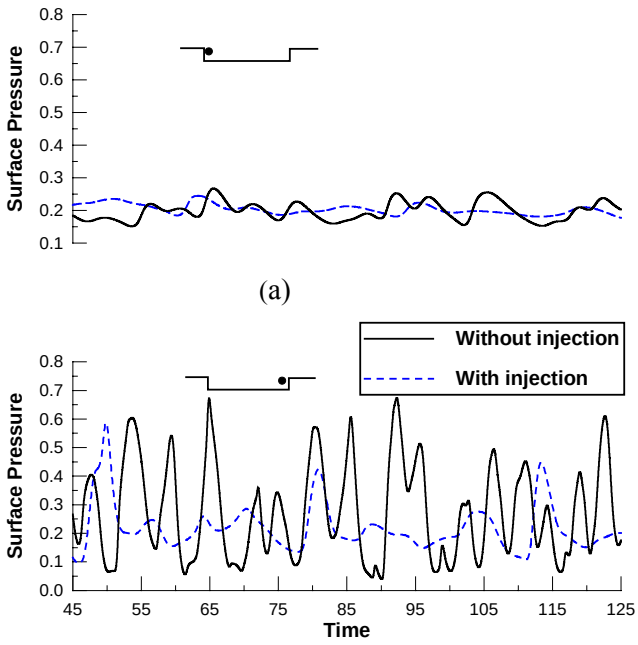

Fig. 6: Pressure oscillations at (a) the fore wall and (b) the aft wall locations, with and without injection

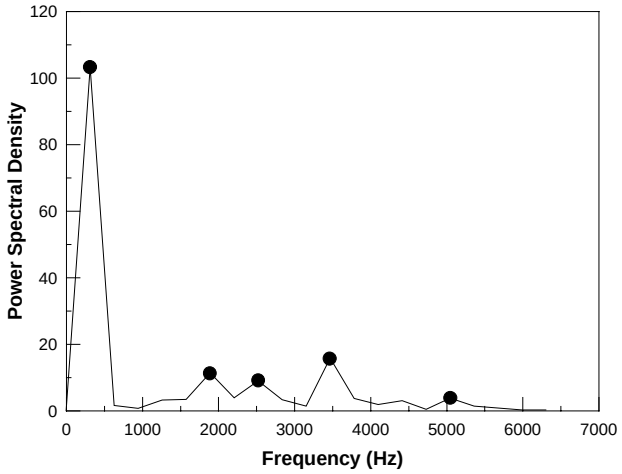

Fig. 7: The dominant frequencies for the cavity flow with injection.

Figures 8 and 9 show snapshots of vorticity and pressure contours, respectively, at three different times ($\Delta t_c = 0.75$). The thickness of the shear layer increases due to the upstream injection. This increase could significantly reduce the amplitude of cavity oscillations[9]. The predicted results show the suppression of the roll up or downward deflection of the shear layer due to the increase in its thickness.

This is consistent with the experimental observations.

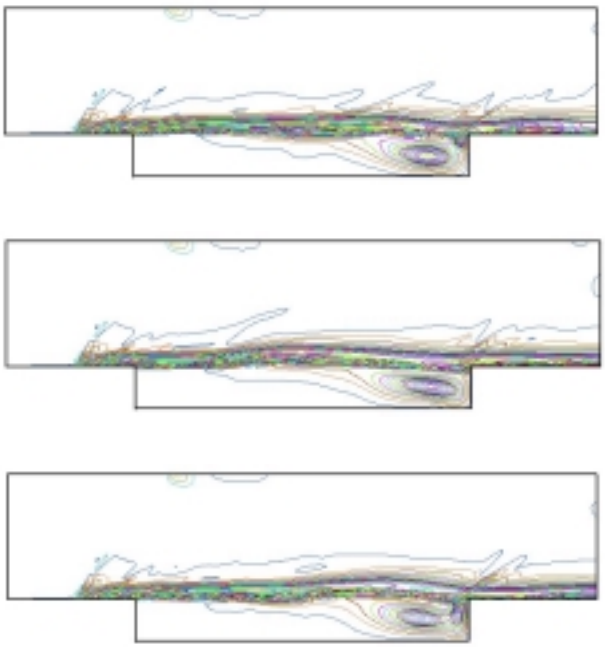

Fig. 9: Snapshots of vorticity contours for the cavity flow with an upstream injection; $J = 1$, $M = 2.0$, and $L/D = 7.76$.

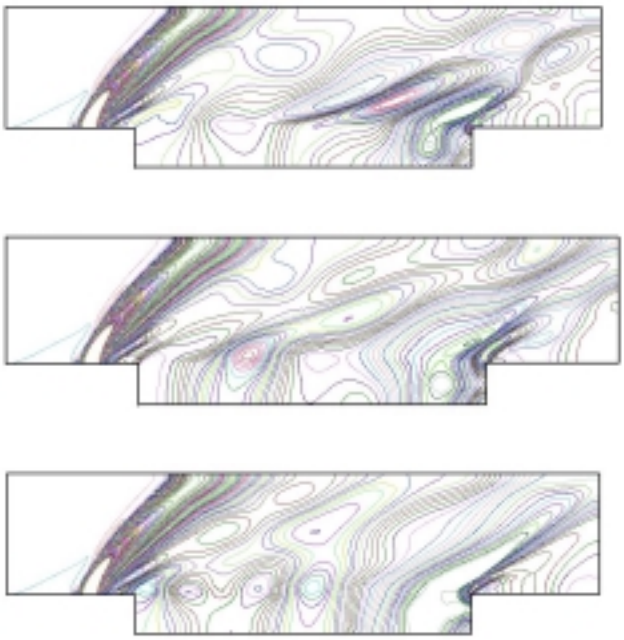

Fig. 8: Snapshots of pressure contours for the cavity flow with an upstream injection; $J = 1$, $M = 2.0$, and $L/D = 7.76$.

5. Concluding remarks

In the present paper, we use the CESE method to simulate supersonic flows over open cavities in the setting of advanced scramjet engine combustor. Both Euler and Navier Stokes solvers are used and three testing conditions are simulated. The calculated results showed that the CESE method could predict the well-known feedback mechanism and the self-sustained oscillations in the cavity flows. We have shown that the CESE method could catch the dominant frequencies up to the fourth mode in the AF Case, and to the fifth mode for cavity flow with injection. We observed that oscillation pattern changes from cycle to cycle, which was also reported by experimentalists. Finally, preliminary results shows that an upstream injection could drastically suppress flow oscillations and simultaneously cause the dominant frequencies shifted to lower values. The above results show that the CESE method is indeed a viable CFD method for high fidelity simulation of unsteady flows relevant to advanced scramjet engines.

6. Acknowledgement

This work was funded by the AFSOR, USAF, under grant number F49620-01-1-0051. The

References

1. M.R. Gruber, R.A. Baurle, , T. Mathur, and K.-Y. Hsu, "Fundamental Studies of Cavity-Based Flame holder Concepts for Supersonic Combustors," the 35th AIAA/ASME/SAE/ASEE Joint Propulsion Conference, Los Angeles California, June 1999.

2. M.R. Gruber, K. Jackson, T. Mathur, F. Billig, "Experiments with a Cavity-Based Fuel Injector for Scramjet Applications," the XIV International Society of Air-Breathing Engines, Florence Italy, September 1999.

3. K. Yu, K.J. Wilson, R.A. Smith, and K.C. Schadow, "Experimental Investigation on Dual-Purpose Cavity in Supersonic Reacting Flow," AIAA 98-0723, the 36th Aerospace Sciences Meeting & Exhibit, Reno NV, January 1998.

4. R.A. Baurle, C.-J. Tam, and S. Dasgupta, "Analysis of Unsteady Cavity Flows for Scramjet

Applications," AIAA 2000-3617, the 36th AIAA/ASME/SAE/ASEE Joint Propulsion Conference, Huntsville Alabama, July 2000.

5. A. Ben-Yakar and R. K. Hanson, " Cavity Flame-Holders for Ignition and Flame Stabilization in Scramjets: An Overview," Journal of Propulsion and Power, Vol. 17, No. 4, 2001, pp. 869-877.
6. H.H. Heller, D.G. Holmes, and E.E. Covert, " Flow-Induced Pressure Oscillations in Shallow Cavities," Journal of Sound and Vibration, Vol. 18, No. 4, 1971, pp. 545-553.
7. D. Rockwell and E. Naudascher, " Review – Self-Sustaining Osciallations of Flow Past Cavities," Vol. 100, 1978, pp. 152-165.
8. X. Zhang, " Compressible Cavity Flow Oscillation due to Shear Layer Instabilities and Pressure Feedback," AIAA Journal, Vol. 33, No. 9, 1995, pp. 1404-1411.
9. A.D. Vakili and C. Gauthier, " Control of Cavity Flow by Upstream Mass-Injection," Journal of Aircraft, Vol. 31, No. 1, 1994, pp. 169-174
10. R.L. Sarno and M.E. Franke, " Suppression of Flow-Induced Pressure Oscillations in Cavities," Journal of Aircraft, Vol. 31, No. 1, 1994, pp. 90-96
11. A.M. Lamp and N. Chokani, " Computation of Cavity Flows with Suppression Using Jet Blowing," Journal of Aircraft, Vol. 34, No. 4, 1997, pp. 545-551
12. S.-C. Chang, "The Method of Space-Time Conservation Element and Solution Element – A New Approach for Solving the Navier Stokes and Euler Equations," Journal of Computational Physics, Vol. 119, 1995, pp. 295-324.
13. S.-C. Chang, S.-T. Yu, A. Himansu, and X.-Y. Wang, " The Method of Space Space-Time Conservation Element and Solution Element – A New Paradigm for Numerical Solution and Conservation Laws," Computational Fluid Dynamics Review 1997, John Wiley and Sons, UK.
14. S.-C. Chang, X.-Y. Wang, and C.-Y Chow, "The d of Space-Time Conservation Element and Solution Element – A New High Resolution and Genuinely Multidimensional Paradigm for Solving Conservation Laws," Journal of Computational Physics, Vol. 156, 1999, pp. 89-136.
15. S.-C Chang, X.-Y Wang, and W.-M. To, " Application of the Space-Time Conservation Element and Solution Element Method to One-Dimensional Covection-Diffusion Problem," Journal of Computational Physics, Vol. 165, 2000, pp. 189-215.
16. R.L. Jr. Stallings and F.J. Wilcox, " Experimental Cavity Pressure Distributions at Supersonic Speeds," NASA TP-2683, June 1987.